Chemical Engineering & Processing: Process Intensification 226 (2026) 110880

Contents lists available at ScienceDirect

Chemical Engineering and Processing - Process Intensification

journal homepage: www.elsevier.com/locate/cep

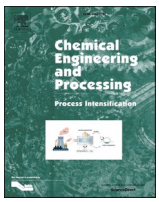

Thermodynamic study of SO_2 reactive absorption into H_2SO_4/H_2O_2 aqueous solutions for Intensified Tail-Gas Scrubbing in Sulfuric Acid Plants

D. Flagiello [a,*], F. Di Natale [a], A. Lancia [a], I. Sebastiani [b], M. Verri [b], A. Erto [a]

[a] Department of Chemical, Materials and Production Engineering, University of Naples, Federico II, P.le Tecchio, 80 - 80125 Naples, Italy
[b] Ballestra SpA, Via Piero Portaluppi 17 - 20138 Milan, Italy

ARTICLE INFO

Keywords:
Sulfuric acid production plant
Double contact double absorption
SO_2 Oxidative scrubber
Hydrogen peroxide tail scrubber
Thermodynamic modelling
ASPEN PLUS®V.14

ABSTRACT

This study investigates the thermodynamics of SO_2 absorption in aqueous H_2SO_4 solutions (30 and 60 % w/w) doped with H_2O_2 up to 1.8 g/L, aiming to enable a reactive oxidative scrubbing process for flue gas treatment. Absorption tests were carried out at 20 and 50 °C in a lab-scale fed-batch bubble column, over a range of SO_2 concentrations from 100 to 3000 ppm_v. The results show that H_2O_2 significantly increases SO_2 solubility via fast gas-liquid reaction forming H_2SO_4. Despite the expected decrease in physical solubility with increasing temperature, oxidative absorption remains efficient due to reaction enhancement. Equilibrium data were used to validate a thermodynamic model in ASPEN PLUS® V.14, which accounts for gas-liquid and chemical equilibria using the Elec-NRTL method. The model provides the thermodynamic foundation required for the design of continuous oxidative scrubbers for tail-gas treatment in sulfuric acid plants. When coupled with appropriate mass-transfer and reaction-kinetic models, the developed equilibrium framework enables the estimation of column size, liquid and reagent consumption and overall process performance, supporting compliance with increasingly stringent EU SO_2 emission standards while minimizing CAPEX and layout modifications, particularly in retrofit applications compared to alternative technologies.

1. Introduction

Abatement of sulfur oxides in flue gases is still a significant industrial concern. Sulfur oxides (SO_x) are polluting and dangerous gaseous species commonly found in exhaust gases from power plants, industrial boilers, metallurgical furnaces, mineral processing, sulfuric acid production plants, as well as some chemical plants using $H_2SO_{4(aq)}$ for organic and inorganic chemical production [1,2]. Efficient flue-gas desulfurization can be achieved mainly by means of wet-scrubbing techniques using traditional state-of-the-art methods [3,4]. Due to the progressive lowering of permissible emission limits, more effective scrubbing technologies, i.e. Wet Oxidative Scrubbing (WOS), which include the use of oxidizing reagents, can be adopted to provide more efficient gas cleaning and to reduce plant size [5–7]. On the other hand, these processes produce liquid effluents, which must be treated correctly or disposed of, if they are not marketable. Among the available options, an oxidative process using aqueous solutions of hydrogen peroxide appears to be very attractive for desulfurization [8–10], as it results in the production of valuable sulfuric acid without generating any other effluent. This treatment finds an interesting application in industrial processes devoted to the production of sulfuric acid, as fairly concentrated sulfuric acid stream produced by the oxidative reaction [8,10] according to the following reaction:

$$SO_{2(aq)} + H_2O_{2(l)} \rightarrow H_2SO_{4(aq)} \quad (1)$$

which is readily mixed with the main product stream; in such a way, the overall plant efficiency increases, contrary to conventional scrubber processes, where the removal of unconverted SO_2 from the tail gas results in the production of a liquid effluent requiring further treatment.

The large-scale production of sulfuric acid is predominantly based on the Double Contact Double Absorption (DCDA) process [11], which involves two catalytic stages of SO_2 oxidation to SO_3, followed by two absorption towers where SO_3 is captured and converted into concentrated sulfuric acid (98 - 99 %). This configuration achieves high conversion efficiencies, typically greater than 99.7 % and ensures very low final SO_2 emissions (< 420 ppm_v), making it the current industrial standard (Directive IED 2010/75/UE) [1,11]. However, the increasingly strict emission limits set in Directive IED 2024/1785/UE, as well as possible additional restrictions imposed by local authorities envisage a

* Corresponding author.
E-mail address: domenico.flagiello@unina.it (D. Flagiello).

https://doi.org/10.1016/j.cep.2026.110880
Received 29 December 2025; Received in revised form 20 April 2026; Accepted 17 May 2026
Available online 20 May 2026

future request for even lower emission limits. In this context, an oxidative absorption column (Hydrogen Peroxide Tail Scrubber) can be adopted, in which the residual SO_2 is oxidized directly to sulfuric acid by contacting it with a recirculating solution of diluting H_2SO_4 with addition of H_2O_2 (Fig. 1) prompting the reaction shown in Eq. (1). The addition of hydrogen peroxide represents a convenient choice both in the case of a new project where very low emissions are required and as a retrofit solution in existing plants being subject to revised, lower emission limits.

Pilot and full-scale studies have demonstrated that a well-designed H_2O_2-based oxidative scrubber can achieve emissions as low as 50 mg/Nm^3 [2,12,13] thus complying with emerging EU standards. In addition, whenever retrofitting of an existing plant is being considered, this solution involves both minimal plant modifications if compared to process enhancement solutions (e.g. installation of an additional SO_2 catalytic conversion stage and cesium based catalyst) and a leaner, more environmentally sound choice if compared to other scrubbing technologies such as caustic or ammonia-based scrubbers generating a sulfite solution as liquid effluent that cannot be disposed [3,4,14,15]. The main advantage of using hydrogen peroxide is the conversion of SO_2, which would otherwise be lost in the tail gas, into valuable sulfuric acid with a non-negligible reduction of the OPEX of the scrubber. Vice versa, the effluent generated by scrubbers designed to use caustic soda or ammonia must be further treated before disposal or, alternatively, to be converted to a sellable product [16,17].

However, unlike catalytic converters of DCDA, no consolidated design standard currently exists for oxidative scrubbers at industrial scale. The success of the technology hinges on several critical factors: reactive stability and minimization of H_2O_2 decomposition, optimized balance between reagent dosage, contact time, mass transfer and gas-liquid reaction rate.

Colle et al. [2] investigated the kinetics of SO_2 absorption in H_2SO_4–H_2O_2 solutions, highlighting the role of interfacial mass transfer coefficients and the enhancement effect of the fast liquid-phase reaction. Colle et al. [9] also proposed practical enhancement factors for scrubber design, though valid over a limited operating range. More recent experiments conducted by Shostak et al. [18] have explored the oxidation of H_2SO_3 to H_2SO_4 via H_2O_2, while Flagiello et al. [8] developed a rigorous gas-liquid reaction kinetic model based on the Hatta number and also provided new thermodynamic data relevant for reactor design. Liémans et al. [12] further confirmed that SO_2 absorption in H_2O_2-containing systems is an efficient route to direct H_2SO_4 formation in packed liquid columns.

Although promising results are available in the literature, this technology still requires further technical and scientific investigation, e.g. about the stability of the reagent, which plays a key role in process feasibility, as H_2O_2 is prone to decomposition in acidic and corrosive environments. Therefore, continuous monitoring of ORP (Oxidation-Reduction Potential) and pH, along with precise dosing, is necessary to prevent waste and unnecessary cost increases. However, the most critical aspects include the thermodynamics of the process (particularly the effects of temperature, H_2O_2 dosage and acidity in the presence of sulfuric acid), which is essential to support the modelling of kinetic data and the rigorous formulation of reliable design equations, and the gas–liquid reaction kinetics. In fact, despite the growing interest in H_2O_2-based oxidative scrubbing, a consistent thermodynamic dataset for the H_2SO_4–H_2O_2–SO_2 system at industrially relevant acid strengths is still lacking in the open literature [1,19] while most of the available data are published using only hydrogen peroxide in aqueous solutions [8] and other very general information can be found in patents already applied for metallurgical processes [10].

In this context, the present work provides new equilibrium solubility data for SO_2 in H_2SO_4–H_2O_2 solutions over a range of temperatures (T = 20 and 50 °C), acid concentrations (C_{H2SO4} = 30 % and 60 % w/w) and oxidant dosages (C_{H2O2} = 0.6 to 1.8 g/L) relevant for tail-gas treatment in sulfuric acid plants, covering a wide range of SO_2 gas inlet concentrations ($C_{SO2(g),in}$ = 100 to 3000 ppm_v). Absorption experiments were conducted in a laboratory-scale bubble column operated in fed-batch mode, enabling time-resolved monitoring of SO_2 absorption until liquid saturation. The use of a fed-batch bubble column was intentionally selected to quantitatively determine the sulfur content at equilibrium condition, equivalent to the SO_2 absorbed and converted into sulfates, according to Eq. (1). In addition, a thermodynamic equilibrium model based on the Elec-NRTL method, vapor-liquid equilibrium and chemical reaction equations has been implemented in ASPEN PLUS® V. 14 and validated against the experimental dataset. The resulting thermodynamic framework enables a consistent evaluation of gas-liquid equilibrium and the associated mass transfer driving force, while being inherently limited to equilibrium calculations and process feasibility assessment. When coupled with mass transfer and reaction kinetic models, it can be effectively applied to the simulation and design of industrial gas-liquid contactors, thereby bridging fundamental thermodynamics and practical engineering applications.

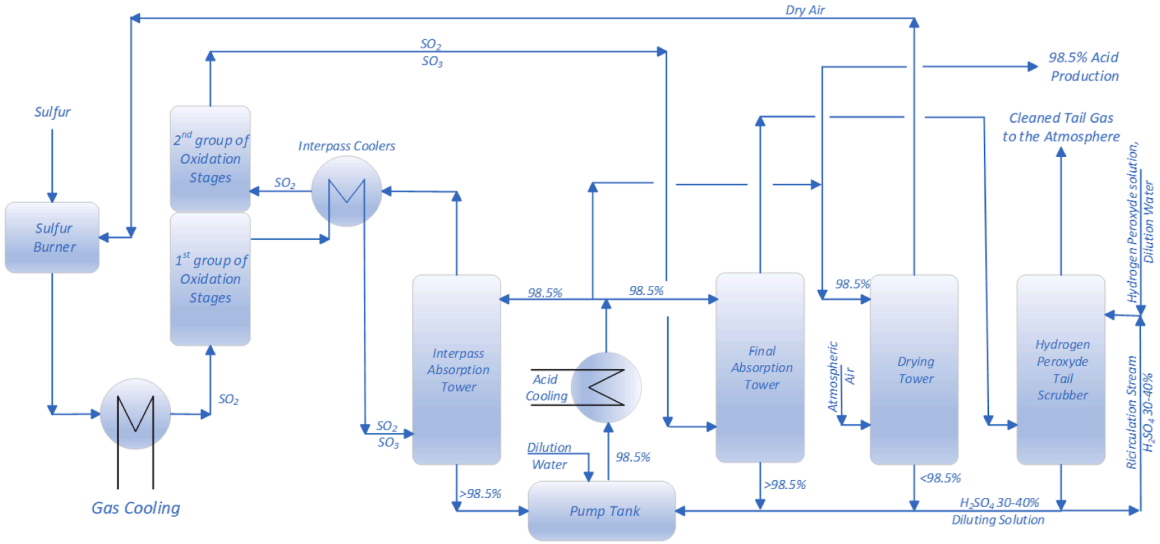

Fig. 1. Process flow diagram (PFD) of a sulfuric acid production plant with integrated WOS (Hydrogen Peroxide Tail Scrubber).

2. Materials and methods

2.1. Materials

High pressure cylinders of pure N_2 at 5.0 technical grade and SO_2 at 3000 ppm_v in N_2 (Rivoira Gas, Italy) were used for simulated flue-gas production; Sulfuric acid (H_2SO_4) aqueous solution at 98 % w/w, hydrogen peroxide (H_2O_2) aqueous solution at 30 % w/w and distilled water to dilute the acid solution (Sigma Aldrich, Italy) were used to prepare the absorbing liquids for the experiments.

2.2. Experimental set-up

The experiments to determine the solubility dataset of SO_2 in sulfuric acid solution containing different dosages of H_2O_2 were performed in a fed-batch bubble absorber for equilibrium tests. This experimental set-up is fully instrumented with flow meters, temperature and pressure controllers as shown in Fig. 2.

This unit is a dynamic liquid-gas contactor and consists of a Pyrex glass column (overall height 0.2 m; internal diameter 0.025 m; thickness 2 mm) where the gas is continuously fed while a finite volume of the absorbing solution is injected in the column as batch phase when the test starts and it is not altered throughout the duration of the test (batch conditions). The injection of solution is made through the valve-syringe system, which is equipped with a luer-lock inlet system at the top of the column. The model flue gas stream fed to the bubble column consists of a mixture of gases available in high-pressure cylinders, which are mixed before the column inlet. It is formed by nitrogen with a variable $SO_{2(g)}$ concentration from 100 up to 3000 ppm_v. Their flow rates are controlled using digital flow meters by SMC Corporation (0 - 20 NL/min; detection limit of 0.1 L/min; and deviation 0.1 % of the full scale of the instrument) to achieve the desired concentration in each test. The gas stream flows through a porous sintered glass gas diffuser (P2 porosity class) to obtain bubble sizes around 4 to 20 μm. This allows a significant improvement in gas-liquid contact so to reduce the time for reaching the equilibrium condition. During the experiments, the liquid is kept at the desired temperature for each test by a thermoregulating system consisting of external water circulation in a column jacket (internal diameter 0.04 m and thickness 2 mm) connected to a thermostatic bath (HAAKE DC 10), to perform tests at constant temperature.

At the column outlet, the gas is sent to a chamber to collect the entrained liquid droplets and any other condensates before to be sent to the gas analysis system. The concentration of SO_2 in the gas stream at the column outlet is checked over time using a Pollutek Gas Analysis system (eGAS-200R UV-DOAS dual range 0 - 600 / 0 - 4000 ppm_v; detection limit of 0.1 ppm_v; and deviation 1 % of the full scale of the instrument). It is worth noting that prior to feeding the gas to the analytical cell of the gas analyzer, the gas is dried by a quenching unit to obtain concentration values on a dry-basis. Further details on the instruments and equipment are given in our former works [20,21]. At the end of the test, the temperature and pH of the exhaust liquid can be measured with a HOBO® digital pH-meter (PCE-228 model).

The experimental activity consists of absorption tests performed in a lab-scale bubble column operating in fed-batch mode at constant temperature $T = 20$ and 50 °C to determine the solubility dataset of SO_2 in concentrated sulfuric acid aqueous solutions at 30 and 60 % w/w with the addition of H_2O_2 at different dosages, so to promote the gas-liquid oxidation reaction with formation of sulfates. The experiments are carried out using a gas flow rate $G_v = 2$ L/min and a finite liquid batch volume $L_{v,batch} = 10$ mL. The scrubbing liquid is represented by sulfuric acid aqueous solutions at 30 and 60 % w/w with addition of hydrogen peroxide from 0 up to 1.8 g/L. The mass concentrations of H_2O_2 used in the equilibrium experiments and dosage are summarized in Table 1.

It should be noted that the H_2O_2 mass concentrations are different for the two sulfuric acid solutions investigated due to their different density

Table 1
Dosage and mass concentration of H_2O_2 used in the absorption experiments with sulfuric acid solutions at 30 and 60 % w/w.

	H_2SO_4[% w/w]	H_2O_2[g/L]	H_2O_2[% w/w]
H_2SO_4–30 %	30	0.6, 0.7, 0.9, 1.2, 1.8	0.05, 0.06, 0.08, 0.10, 0.15
H_2SO_4–60 %	60	0.6, 0.7, 0.9, 1.2, 1.8	0.04, 0.05, 0.06, 0.08, 0.12

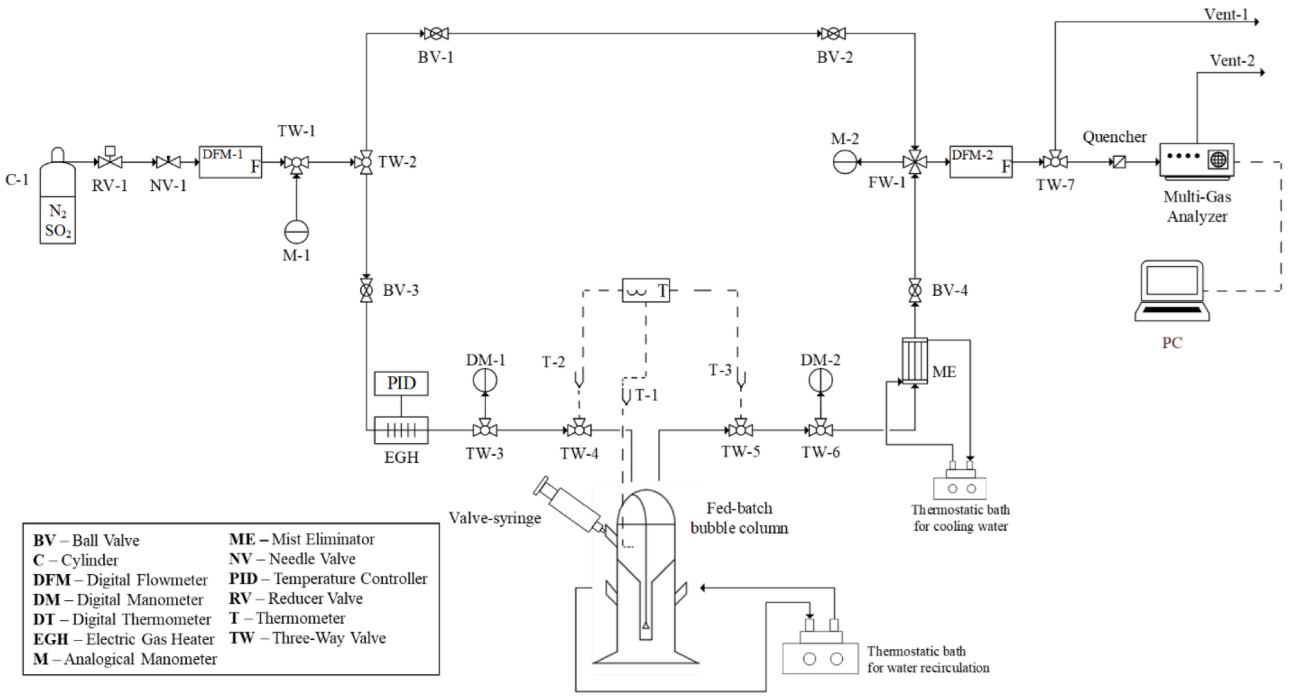

Fig. 2. Process flow diagram (PFD) of the fed-batch bubble column lab-scale.

and molecular weight (1.21 g/mL and 23.86 g/mol for H_2SO_4–30 %, while 1.49 g/mL and 35.31 g/mol for H_2SO_4–60 %); for this reason the H_2O_2 dosage expressed in g/L was also reported in the table. The experimental procedures adopted follow the same approach proposed by Flagiello et al. [4,8]. During the tests, the absorbing solution (batch) is able to absorb $SO_{2(g)}$ over time, up reaching the saturation limit (corresponding to saturation time, t_{sat}), i.e. when $C_{SO2(g),out}$ coincides with the inlet gas value. In this final condition, the amount of $SO_{2(g)}$ absorbed, including both the fraction physically solubilized ($SO_{2(aq)}$) and its fraction converted into sulfates (SO_4^{2-}) in the liquid, corresponds to the total sulfur concentration ($x_{S(eq)}$) in the liquid-phase, which is in equilibrium with the concentration of $SO_{2(g)}$ in the outlet gas ($C_{SO2(g),out}$ @ t_{sat} = $C_{SO2(g),in}$ = $C_{SO2(eq)}$).

2.3. Data analysis

The experimental data obtained in the fed-batch bubble absorber over time ($C_{SO2(g),out}$ (t)) were used to calculate the solubility dataset ($C_{SO2(eq)}$ - $x_{S(eq)}$). The $x_{S(eq)}$ [g/g] is expressed as the ratio of total mass of $SO_{2(g)}$ absorbed from the gas to the total mass of the absorbing solution. To this end, a differential mass balance equation referred to the gas-phase, over time up to saturation time of the solution (t_{sat} [s]) was used to calculate the total concentration of $SO_{2(g)}$ absorbed under thermodynamic equilibrium conditions, as proposed by Flagiello et al. [4,8]:

$$x_{S(eq)} = \frac{G_{m,SO_2} MW_{sol}}{L_{m,sol}} \int_0^{t_{sat}} \left(1 - \frac{C_{SO_{2(g),out}}}{C_{SO_{2(g),in}}}\right) dt = x_{SO_2} + x_{SO_4^{2-}} \quad (2)$$

where $G_{m,SO2}$ [g/s] is the mass flow rate of $SO_{2(g)}$ fed at bubble column, MW_{sol} [g/mol] is the molecular weight of the absorbing liquid solution, $L_{m,sol}$ is its mass (batch) [g], x_{SO2} [mol/mol] is the mole fraction of SO_2 physically solubilized and x^{2-}_{SO4} [mol/mol] is the mole fraction of SO_2 converted to sulfates.

2.4. ASPEN PLUS modelling

To calculate the solubility data of $SO_{2(g)}$ in H_2SO_4–H_2O_2 aqueous solution at different concentrations, temperatures and pressures investigated in the present work, a thermodynamic equilibrium model was developed in ASPEN PLUS® V.14 simulator and validated by comparison with experimental results. The model prediction of SO_2 solubility data ($C_{SO2(eq)}$ - $x_{S(eq)}$) is based on an equation code that accounts for the entire absorption mechanism of $SO_{2(g)}$ in H_2SO_4–H_2O_2 aqueous solutions, including gas-liquid phase equilibria and chemical reaction equilibria in liquid-phase.

The proposed calculation code allows to simultaneously solve the mass and energy balances in a continuous unit using a Flash block, which is a thermodynamic equilibrium stage.

In this unit two input streams are fed: a gas consisting of N_2 with defined SO_2 concentration, and a liquid consisting of H_2SO_4 aqueous solutions at either 30 % or 60 % w/w with addition of H_2O_2 at experimental dosages. At the output of the Flash block, two streams (gas and liquid) are at thermodynamic equilibrium condition.

The code also includes all the interactions between the chemical species involved in the process, such as gas-liquid phase equilibria (solubility and volatility data) and chemical reaction equilibria in the liquid-phase. The equilibrium equations and the values of the related constants, as a function of the temperature, are given in Table 2.

It should be noted that the constant in Eq. (12), which shows the contribution of the different sulfur species involved in the absorption process, was experimentally calculated by Flagiello et al. [8], while the overall reaction between SO_2 and H_2O_2 expressed by Eq. (1) is given by the sum of reactions in Eq. (10), Eq. (11) and Eq. (12) and the reverse of Eq. (9) multiplied by 2.

Table 2
Set of equations for SO_2 absorption in H_2O_2/H_2SO_4 model aqueous solutions including the values of the gas-liquid (K_{P° and K_H [atm]) and chemical (K_{Eq} [mol/mol]^p) constants as a function of the absolute temperature (T_a [K]) taken from Flagiello et al. [8];[20], Sander et al. [22] and Perry's Chemical Engineers' Handbook [23]. The coefficient p represents the difference between the stoichiometric coefficients of the products and reactants for each chemical reaction considered.

Eqs.	Equilibrium Equations	Constant Equations
(3)	$SO_{2(g)} \rightleftharpoons SO_{2(aq)}$	$LnK_H = 72.45 - \frac{5579}{T} - 8.76Ln(T)$
(4)	$H_2SO_{4(aq)} \rightleftharpoons H_2SO_{4(g)}$	$LnK_H = 16.85 - \frac{8900}{T}$
(5)	$H_2SO_{4(l)} \rightleftharpoons H_2SO_{4(g)}$	$LnK_{P^\circ} = 15.65 - \frac{9748}{T}$
(6)	$H_2O_{2(aq)} \rightleftharpoons H_2O_{2(g)}$	$LnK_{P^\circ} = 70.11 - \frac{8600}{T} - 8.34Ln(T) + 3.9{\cdot}10^{-6}T^2$
(7)	$H_2O_{(l)} \rightleftharpoons H_2O_{(g)}$	$LnK_{P^\circ} = 61.08 - \frac{7206}{T} - 7.14Ln(T) + 4.1{\cdot}10^{-6}T^2$
(8)	$2H_2O_{(l)} \rightleftharpoons H_3O^+ + OH^-$	$LnK_{Eq} = 132.89 - \frac{13446}{T} - 22.48Ln(T)$
(9)	$H_2SO_{4(aq)} + 2H_2O_{(l)} \rightleftharpoons 2H_3O^+ + SO_4^{2-}$	$LnK_{Eq} = -47.72 + \frac{47802}{T}$
(10)	$SO_{2(aq)} + 2H_2O_{(l)} \rightleftharpoons H_3O^+ + HSO_3^-$	$LnK_{Eq} = -5.89 + \frac{637}{T} - 1.5{\cdot}10^{-2}T$
(11)	$SO_{2(aq)} + 3H_2O_{(l)} \rightleftharpoons 2H_3O^+ + SO_3^{2-}$	$LnK_{Eq} = -40.68 + \frac{3467}{T}$
(12)	$HSO_3^- + SO_3^{2-} + 2H_2O_{2(aq)} \rightleftharpoons H_2O_{(l)} + H_3O^+ + 2SO_4^{2-}$	$LnK_{Eq} = 3.95 + \frac{63005}{T}$

A property method was used to calculate the physical and transport properties of all components and the corrective factors of the equilibrium correlations (activity coefficients γ and fugacity coefficients ϕ). In the case of a non-diluted solution, the Electrolyte Non-Random Two-Liquid (Elec-NRTL) model [24,25] was used. In the present case, since the process pressure is 1 atm, the ideal gas approximation was assumed and therefore the fugacity coefficients were set equal to ϕ = 1. The general expression for the calculation of the γ coefficient in the Elec-NRTL model is given by the sum of the excess Gibbs free energies giving rise to three contributions: the Pitzer-Debye-Huckel model expression (Ln (γ)^{PDH}); the NRTL model expression for local interactions (Ln (γ)^{NRTL}); the Born model expression (Ln (γ)^{Born}). The details of the model equations are reported in Chen et al. [24,25] and already implemented in the software database. The Elec-NRTL thermodynamic framework adopted in this work relies on the default ASPEN PLUS® V. 14 electrolyte database, including the binary interaction parameter sets GMELCC-1, GMELCD-1, GMELCE-1 and GMELCN-1. These parameters are automatically retrieved by the software when the corresponding property method and electrolyte pairs are selected, ensuring full reproducibility of the simulations without the need for explicit tabulation.

The calculation routine includes the possibility of varying all thermodynamic parameters of interest to simulate experimental conditions, such as flow rates, composition, temperature and pressure of the input stream, and pressure and temperature of the thermodynamic flash unit. The model solubility data were obtained with a sensitivity analysis tool available in ASPEN PLUS® V.14, i.e. by varying one of the parameters, e. g. the gas composition (concentration of SO_2 in the gas) and fixing the flow rates, temperature, pressure and liquid composition (concentrations of H_2SO_4 and H_2O_2 in the liquid-phase) to be investigated, in order to be able to describe the entire curve in the gas concentration ranges of interest for this work.

3. Results and Discussion

Fig. 3 shows the time evolution of the outlet SO_2 gas concentration in the fed-batch bubble column during a representative experiment, conducted at a gas flow rate $G_v = 2$ L/min with an inlet SO_2 concentration $C_{SO2(g),in} = 945$ ppm_v, and a liquid batch volume $L_{v,batch} = 10$ mL with a hydrogen peroxide concentration $C_{H2O2} = 1.8$ g/L and a sulfuric acid concentration $C_{H2SO4} = 60$ % w/w.

Immediately after liquid injection, a sharp drop in the outlet SO_2 concentration is observed, highlighting a very fast absorption process controlled by gas-liquid reaction kinetics (Eq. (1)), which effectively represents the maximum reaction rate under the investigated conditions. This initial transient is followed by a quasi-steady absorption regime, whose duration and extent are primarily governed by the available H_2O_2 dosage, while all other operating parameters are kept constant. As the oxidizing capacity of the liquid-phase is progressively depleted, the outlet SO_2 concentration gradually increases approaching the gas inlet concentration value. This asymptotic behavior indicates that thermodynamic equilibrium has been reached, with the liquid phase approaching saturation in sulfur species, beyond which further absorption is no longer possible.

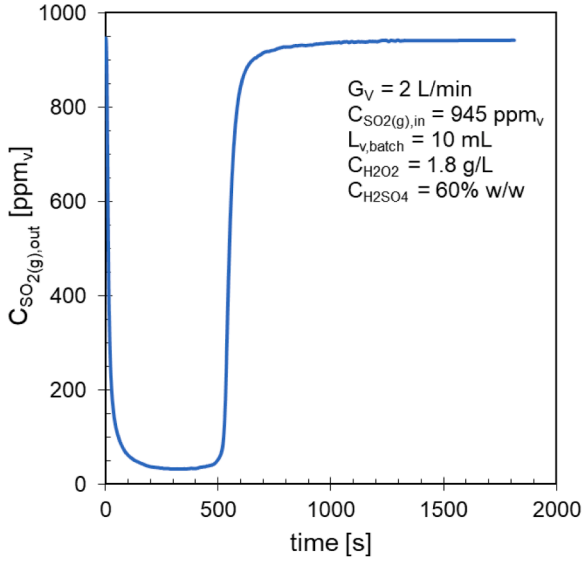

Fig. 3. Time evolution of the outlet SO_2 gas concentration in the fed-batch bubble column during a representative experiment: $G_v = 2$ L/min; $C_{SO2(g),in} = 945$ ppm_v; $L_{v,batch} = 10$ mL; $C_{H2O2} = 1.8$ g/L; $C_{H2SO4} = 60$ % w/w.

As described in the Materials and Methods section and consistently adopted in the Authors' previous works [4,8], the equilibrium solubility is determined by integrating the area above the $SO_{2(g)}$ concentration vs time curve according to the mass balance (Eq. (13)), thereby obtaining a dataset of the absorbed amount at saturation for each test. In Fig. 4, the experimental and model prediction results of SO_2 solubility in H_2SO_4 aqueous solutions at 30 % and 60 % w/w are shown for each H_2O_2 dosage investigated (see Table 1), at $T = 20$ °C and $P = 1$ atm.

The experimental data in the presence of H_2O_2 have the typical trend of a chemical absorption, with a horizontal line coinciding with the x-axis and the ascending branch of the equilibrium curves overlapping the physical solubility curve in H_2SO_4 aqueous solutions, apart from the shift towards higher total sulfur mass fractions in the liquid-phase due to the oxidative absorption contribution given by the presence of H_2O_2. Compared to the solubility values found in sulfuric acid solutions (without H_2O_2), which show good agreement with the data reported by Thomas et al. [1], the experimental results in Fig. 4 show that the addition of the oxidant gives a significant increase in $SO_{2(g)}$ solubility: as expected, the solubility increases by increasing H_2O_2 dosage because the gas-liquid reaction of oxidation to sulfuric acid of SO_2 is promoted (Eq. (1)). In fact, when $SO_{2(g)}$ concentration is 3000 ppm_v, and H_2O_2 is added at 0.6 g/L, a significant increase in SO_2 solubility is observed, which is of the order of 13.6 times compared to the test with only H_2SO_4 at 30 % w/w and approximately 18.6 times for H_2SO_4 at 60 % w/w. Furthermore, an increase in H_2O_2 concentration leads to further increases in SO_2 solubility: for instance, with a 3000 ppm_v SO_2 concentration in the gas, the addition of H_2O_2 at 0.7 g/L in H_2SO_4 aqueous solutions at 30 % w/w gives a solubility of about 1.2 times compared to the solution with H_2O_2 at 0.6 g/L, whereas with a concentration of 1.8 g/L, a solubility value of about 3 times is obtained. On the other hand, for H_2SO_4 solutions at 60 % w/w, an increase in solubility of about 1.2 times is still observed using H_2O_2 at 0.7 g/L compared to the solution with H_2O_2 at 0.6 g/L, whereas with concentration of 1.8 g/L, a solubility value of about 2.8 times is achieved. This decrease in solubility is mainly due to the presence of sulfuric acid in solutions, which inhibits the gas-liquid reaction (Eq. (1)) as the reaction product is present in larger amounts

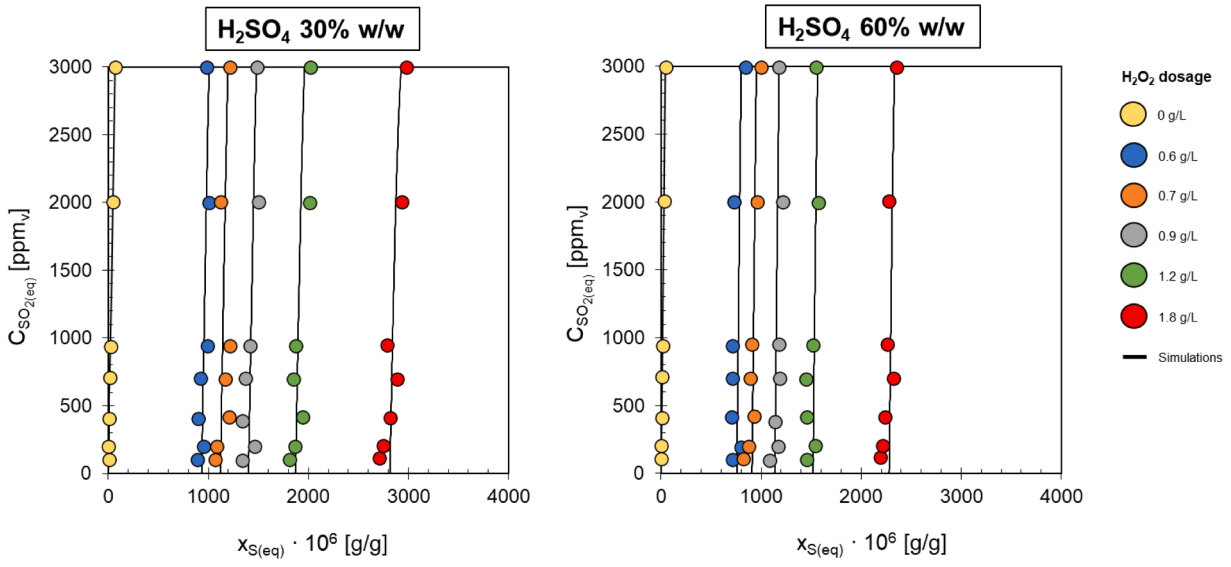

Fig. 4. Solubility dataset expressed as concentration of SO_2 in the gas-phase ($C_{SO2(eq)}$) as a function of the mass fraction of total sulfur in the liquid-phase ($x_{S(eq)} \bullet 10^6$) for SO_2 absorption at $T = 20$ °C and $P = 1$ atm in H_2SO_4 aqueous solutions at 30 and 60 % w/w and different H_2O_2 dosages (see Table 1). The simulation results in ASPEN PLUS® are also shown as a solid line.

rising from 30 to 60 % w/w. The results also show that the prediction model, developed with the ASPEN PLUS®, provides a very good estimate of the experimental solubility data at 20 °C for all H_2O_2 dosages investigated in both the sulfuric acid solutions within the region of SO_2 concentration in the gas-phase (from 100 to 3000 ppm_v) with a coefficient of determination (R^2) greater than 0.96.

To extend the comparison and ensure a consistent evaluation of oxidative absorption performances, the model solubility data obtained in our former work (Flagiello et al. [8]) with a dosage of $H_2O_{2(aq)}$ that ranged from 0.6 to 1.2 g/L are also reported. In those experiments, the oxidation effect of SO_2 in the liquid-phase was studied in H_2O_2 solution without sulfuric acid; the comparison aims at quantifying the solubility differences measured in a H_2O_2 aqueous system not inhibited by the presence of $H_2SO_{4(aq)}$ compared to the equivalent values in the two absorbing solutions tested in the present work (H_2O_2/H_2SO_4–30 % and H_2O_2/H_2SO_4–60 %).

Fig. 5 reports the model-derived mass solubility values of total sulfur in the absorbing liquid ($x_{S(eq)}$) using a bar-chart representation to facilitate a direct comparison of the effects of H_2SO_4 (0, 30 and 60 % w/w) H_2O_2 (0.6, 0.7, 0.9 and 1.2 g/L) and SO_2 (100, 1000, 2000 and 3000 ppm_v) concentrations. Although based on the same validated thermodynamic framework presented in the previous figure, this format highlights the relative influence of the main operating variables and improves the readability of comparative analysis.

In Fig. 5, a significant decrease in SO_2 solubility in the presence of $H_2SO_{4(aq)}$ from 0 up to 60 % w/w can be observed for each different $H_2O_{2(aq)}$ dosage investigated. This effect decreases by increasing SO_2 concentration in the gas-phase and increases by increasing $H_2O_{2(aq)}$ dosage. In addition, the decrease in solubility as the concentration of SO_2 in the gas-phase decreases is much more pronounced with the absorbing solution containing only H_2O_2, whereas when sulfuric acid is added at 30 % and 60 % w/w, this decrease seems to be less pronounced and the solubility values are about constant. In this case, the dependence of the solubility on the SO_2 concentration in the gas-phase is very low, due to the greater slope of the ascending branch (corresponding to physical absorption section) of the equilibrium curves, which in the case of the H_2O_2/H_2SO_4–30 % and H_2O_2/H_2SO_4–60 % solutions are almost vertical (proportional to the slopes observed for only sulfuric acid) as observed in Fig. 4. On the contrary, for H_2O_2 absorbing solution, the slope was similar to the SO_2 absorption in water (see data by Flagiello et al. [8]). In the case of the minimum tested dosage of $H_2O_{2(aq)}$ (0.6 g/L), compared to H_2O_2 solution, the decrease in solubility in H_2O_2/H_2SO_4–30 % solution is in the range 18 - 36 % while it is about 35 - 70 % for H_2O_2/H_2SO_4–60 % solution, in the corresponding range of SO_2 concentrations in the gas-phase (100 - 3000 ppm_v). Similarly, in the case of the maximum tested dosage of $H_2O_{2(aq)}$ (1.2 g/L) this decrease is in the range 17 - 26 % for H_2O_2/H_2SO_4–30 % and 33 - 41 % for H_2O_2/H_2SO_4–60 % solutions.

Further experimental tests were carried out at a constant temperature of 50 °C (1 atm), varying the concentration of SO_2 in the gas between 100 and 3000 ppm_v and using the same absorbing solutions H_2SO_4–30 % and H_2SO_4–60 % w/w. However, compared to the tests at 20 °C, a significant increase in the vapor pressures of all solutions due to the temperature increase was observed. Under these operating

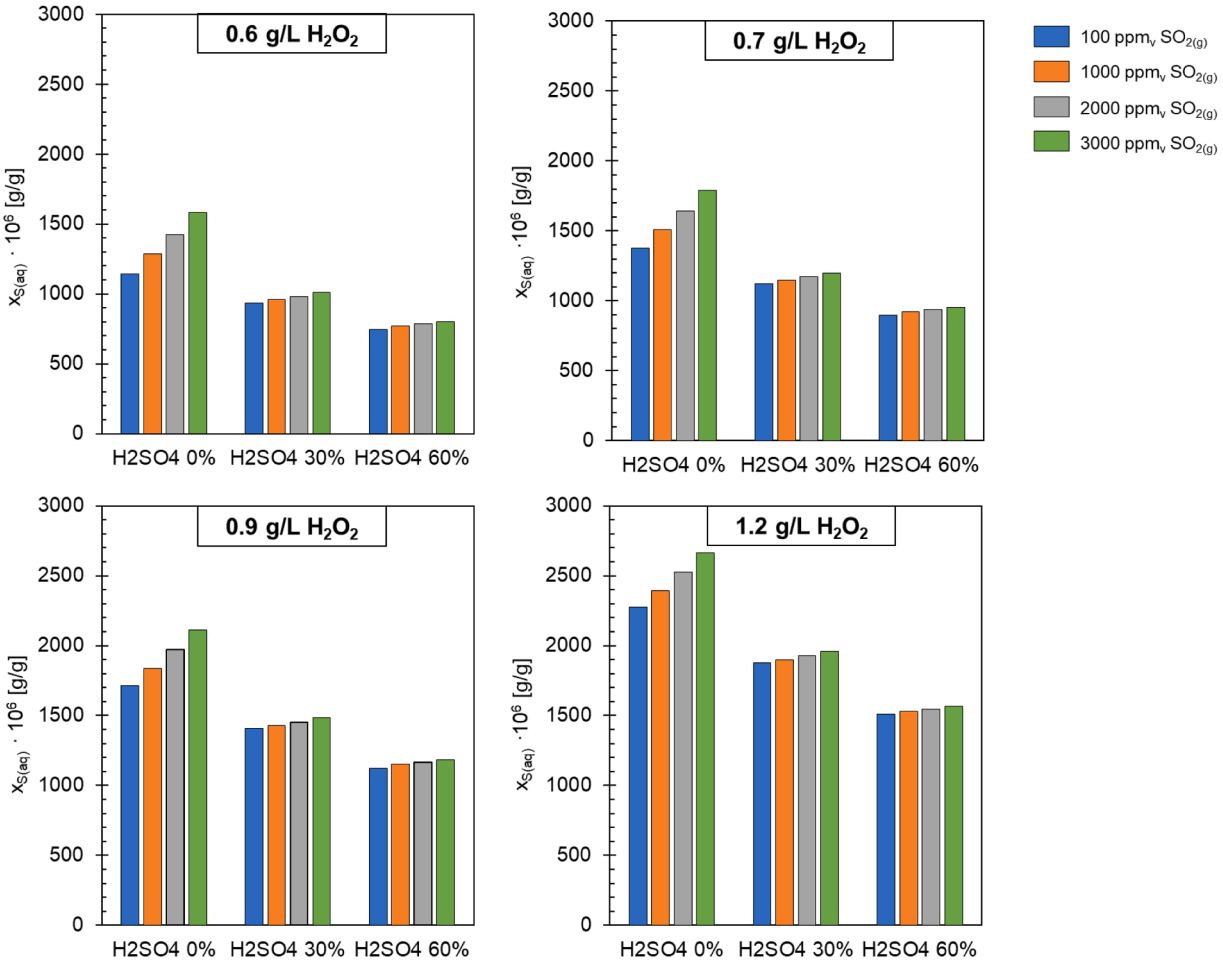

Fig. 5. Comparison of SO_2 solubilities ($x_{S(eq)} \bullet 10^6$) in three different absorbing liquids, i.e. (H_2O_2/H_2SO_4–0 %, H_2O_2/H_2SO_4–30 %, and H_2O_2/H_2SO_4–60 %), parametric at four levels of SO_2 concentration in the gas-phase (100, 1000, 2000 and 3000 ppm_v) and for four H_2O_2 dosages: 0.6 g/L, 0.7 g/L, 0.9 g/L and 1.2 g/L.

conditions, evaporative effects become non-negligible, unlike what was observed in the tests conducted at $T = 20$ °C and they introduce uncertainty in the experimental results that cannot be compensated for, within the adopted setup. The selective evaporation of the absorbent liquid, which occurs in proportions dictated by the marked difference in vapor pressures of the single components of the mixture ($H_2O > H_2O_2 \gg H_2SO_4$), leads both to a reduction in the liquid volume and to a significant alteration of the original solution composition. As a result, the experimental data would be difficult to interpret and could not be reliably associated with the initial properties of the test solutions. The small amounts of H_2O_2 used in the preparation of the solutions do not meaningfully affect their overall vapor pressure; moreover, the vapor pressure of H_2SO_4 is more than six orders of magnitude lower than that of water at the same temperature. Hence, the solutions with lower H_2SO_4 content are inherently more susceptible to evaporation. This issue becomes more critical when the duration of the experiment increases. The test duration itself rises with increasing H_2O_2 concentration. Indeed, a higher concentration of H_2O_2 enhances the SO_2 absorption capacity of the solution, at fixed gas flow rate and inlet concentration, thus extending the time required to reach thermodynamic equilibrium. At constant gas flow rate, the time of the test is also strongly affected by the SO_2 concentration in the feed gas and decreases as the latter increases. Consequently, when the same experimental matrix adopted at 20 °C is reproduced at 50 °C, the combined influence of the inlet SO_2 gas concentration and of the H_2O_2 concentration in the absorbing solution produces varying effects on the evaporative behavior and on the resulting variation in liquid volume between the start and the end of each test.

To maintain the variation in liquid volume below 5 %, which is considered sufficiently small to avoid any appreciable influence on the thermodynamic results, empirical verification showed that the test duration should not exceed approximately 2000 s for solutions containing H_2SO_4–60 % w/w and approximately 1100 s for solutions containing H_2SO_4–30 % w/w. For these reasons, although experiments at 50 °C were conducted under almost all the conditions previously investigated at 20 °C, only the experimental results ($C_{SO2(eq)}$ - $x_{S(eq)}$) considered as reliable, namely those obtained with a liquid-volume variation lower than 5 %, are presented in Table 3 (H_2SO_4–30 %) and Table 4 (H_2SO_4–60 %) along with model-derived mass solubility values ($x_{S(eq)}$).

As anticipated, a larger number of reliable data points were obtained using sulfuric acid solution at 60 % w/w compared to the less concentrated formulation. The results reported in Table 3 indicate that at 50 °C the solubility of SO_2 increases with both the H_2O_2 dosage and the SO_2 concentration in the gas-phase. A comparison with the data collected at 20 °C shows that the solubility values at 50 °C are slightly higher, which contrasts with the expected behavior for a purely physical absorption system, where gas solubility typically decreases with increasing temperature. This behavior is attributed to the presence of H_2O_2, which promotes a fast gas-liquid reaction and offsets the reduction in physical solubility, ultimately resulting in higher overall SO_2 solubility. The experimental data collected at 50 °C were compared with ASPEN PLUS® simulations on a qualitative basis. The retained equilibrium points are consistent with the temperature dependence predicted by the thermodynamic model and follow the same linear trend observed at 20 °C. In particular, the 20 °C dataset exhibits a linear relationship with a slope comparable to that expected from Henry's law for SO_2 in sulfuric acid solutions, with the deviation at saturation corresponding to the contribution of chemical absorption. Although fewer in number, the 50 °C data points lie along the same trend, supporting the thermodynamic consistency of the model. However, due to the reduced number of reliable measurements, quantitative model validation was primarily performed using the 20 °C dataset, while the 50 °C results were used to support a qualitative assessment of the temperature effect.

Overall, these results confirm that the equilibrium model developed in this study is capable of accurately describing equilibrium behavior as a function of temperature, gas-phase SO_2 concentration and liquid-phase composition in terms of sulfuric acid concentration and H_2O_2 dosage.

4. Practical implications for process design

From an engineering perspective, the availability of reliable thermodynamic equilibrium data represents a crucial prerequisite for the design and optimization of gas-liquid contact systems operating under reactive absorption conditions. In particular, the equilibrium model allows to determine the driving force for mass transfer, which is a key parameter in process design, and can be readily implemented in rigorous rate-based process simulators (e.g. the RateFrac module in ASPEN PLUS® [21,26]), in which mass transfer and reaction kinetic correlations can be implemented to enable detailed modelling of industrial packed columns.

Alternatively, a classical design approach can be adopted based on the HTU–NTU approach [8,27], in which the Number of Transfer units (NTU) is evaluated from the integration of the mass transfer driving force along the column height and therefore directly depends on the gas-liquid solubility data. In this context, the thermodynamic equilibrium model provided in this work allows for a consistent estimation of NTU under different operating conditions, while the Height of Transfer Unit (HTU) can be determined from mass transfer coefficients and enhancement factors accounting for the effect of chemical reactions [8, 27]. It is important to emphasize that the present model is purely thermodynamic and therefore suitable for equilibrium calculations and process feasibility assessment, whereas the simulation of real gas-liquid contactors requires its integration with mass transfer correlations and kinetic models.

5. Conclusions

In this work, the solubility of $SO_{2(g)}$ in $H_2SO_{4(aq)}$ solutions (30 % and 60 % w/w) doped with $H_2O_{2(aq)}$ was investigated using a bubble absorber operated in fed-batch mode at 1 atm between 20 and 50 °C. The addition of $H_2O_{2(aq)}$ to 30 % and 60 % w/w sulfuric acid solutions resulted in a significant increase in $SO_{2(g)}$ solubility at 1 atm and 20 °C. Furthermore, the solubility decreases with the same dosage of H_2O_2 when the sulfuric acid concentration increases: in particular, the solubility decreases non-linearly when $H_2SO_{4(aq)}$ is added to the aqueous H_2O_2 solution up to 30 % w/w, and then decreases with a linear trend as

Table 3
Dataset of experimental and model solubility values ($x_{S(aq),exp}$ and $x_{S(aq),mod}$ [μg/g]) at 50 °C as a function of SO_2 concentrations in gas-phase and H_2O_2 in liquid-phase for sulfuric acid solutions at 30 % w/w.

H_2SO_4–30 %											
H_2O_2 0.6 g/L			H_2O_2 0.7 g/L			H_2O_2 0.9 g/L			H_2O_2 1.2 g/L		
$C_{SO2(eq)}$ ppm_v	$x_{S(eq),exp}$ μg/g	$x_{S(eq),mod}$ μg/g	$C_{SO2(eq)}$ ppm_v	$x_{S(eq),exp}$ μg/g	$x_{S(eq),mod}$ μg/g	$C_{SO2(eq)}$ ppm_v	$x_{S(eq),exp}$ μg/g	$x_{S(eq),mod}$ μg/g	$C_{SO2(eq)}$ ppm_v	$x_{S(eq),exp}$ μg/g	$x_{S(eq),mod}$ μg/g
3000	1020	1015	3000	1234	1228	-	-	-	-	-	-

Table 4
Dataset of experimental and model solubility values ($x_{S(aq),exp}$ and $x_{S(aq),mod}$ [μg/g]) at 50 °C as a function of SO_2 concentrations in gas-phase and H_2O_2 in liquid-phase for sulfuric acid solutions at 60 % w/w.

H_2SO_4–60 %											
H_2O_2 0.6 g/L			H_2O_2 0.7 g/L			H_2O_2 0.9 g/L			H_2O_2 1.2 g/L		
$C_{SO2(eq)}$ ppm_v	$x_{S(eq),exp}$ μg/g	$x_{S(eq),mod}$ μg/g	$C_{SO2(eq)}$ ppm_v	$x_{S(eq),exp}$ μg/g	$x_{S(eq),mod}$ μg/g	$C_{SO2(eq)}$ ppm_v	$x_{S(eq),exp}$ μg/g	$x_{S(eq),mod}$ μg/g	$C_{SO2(eq)}$ ppm_v	$x_{S(eq),exp}$ μg/g	$x_{S(eq),mod}$ μg/g
3000	825	818	3000	1006	997	3000	1160	1162	3000	1613	1601
2002	716	726	2008	979	973	2004	1223	1213	2005	1595	1582
943	723	730	952	951	945	950	1196	1191	-	-	-
700	700	719	706	870	874	-	-	-	-	-	-
410	698	710	420	952	946	-	-	-	-	-	-

the acid concentration increases up to 60 % w/w. However, an increase in $H_2O_{2(aq)}$ dosage led to an improvement in the oxidative capacity of the solution and absorption performance can be enhanced, also when the $H_2SO_{4(aq)}$ concentration increases. Experimental results at 50 °C confirmed that, under identical experimental conditions, the solubility of SO_2 increased by up to 5 % despite the rise in temperature, an effect attributed to the compensating increase in the gas-liquid reaction rate.

These findings demonstrate the feasibility of process intensification for gas cleaning combined with an integrated process for the tail-gas treatment in sulfuric acid plants.

The thermodynamic model developed in this work provides the equilibrium framework required to describe the H_2SO_4–H_2O_2–SO_2 system and, when integrated with rate-based mass-transfer and reaction kinetic models, supports the design of H_2O_2-based WOS and the prediction of overall process performance. Therefore, this study provides fundamental equilibrium data as essential tools for thorough industrial process design.

CRediT authorship contribution statement

D. Flagiello: Writing – review & editing, Writing – original draft, Software, Methodology, Investigation, Formal analysis, Data curation, Conceptualization. **F. Di Natale:** Writing – review & editing, Validation, Supervision, Resources, Project administration. **A. Lancia:** Writing – review & editing, Supervision. **I. Sebastiani:** Writing – review & editing. **M. Verri:** Writing – review & editing. **A. Erto:** Writing – review & editing, Writing – original draft, Validation, Supervision, Project administration, Funding acquisition, Formal analysis.

Declaration of competing interest

The authors declare that they have no known competing financial interests or personal relationships that could have appeared to influence the work reported in this paper.

Acknowledgements

The authors warmly thank ChemE Vincenzo Giampaolo for the experimental support during his Master's Thesis.

Data availability

Data will be made available on request.

References

[1] D. Thomas, S. Colle, J. Vanderschuren, Kinetics of SO2 absorption into fairly concentrated sulphuric acid solutions containing hydrogen peroxide, Chem. Eng. Process. Process Intensif. 42 (2003) 487–494, https://doi.org/10.1016/S0255-2701(02)00070-3.
[2] S. Colle, D. Thomas, J. Vanderschuren, Process simulations of sulphur dioxide abatement with hydrogen peroxide solutions in a packed column, Chem. Eng. Res. Des. 83 (2005) 81–87, https://doi.org/10.1205/cherd.03115.
[3] R.K. Srivastava, W. Jozewicz, C. Singer, SO2 scrubbing technologies: a review, Environ. Prog. 20 (2001) 219–228, https://doi.org/10.1002/ep.670200410.
[4] D. Flagiello, F. Di Natale, I. Sebastiani, F. Nava, A. Milicia, A. Lancia, A. Erto, Experimental and modelling study of ammonia-based FGD scrubbers, Chem. Eng. Sci. 305 (2025) 121101, https://doi.org/10.1016/j.ces.2024.121101.
[5] D. Flagiello, A. Erto, A. Lancia, F. Di Natale, Advanced flue-gas cleaning by wet oxidative scrubbing (WOS) using NaClO2 aqueous solutions, Chem. Eng. J. 447 (2022) 137585, https://doi.org/10.1016/j.cej.2022.137585.
[6] D. Flagiello, A. Erto, A. Lancia, F. Di Natale, Advanced exhaust-gas scrubbing for simultaneous de-SOx/NOx using a wet oxidative process with integrated washwater treatment, Chem. Eng. Res. Des. 194 (2023) 731–741, https://doi.org/10.1016/j.cherd.2023.05.014.
[7] D. Flagiello, A. Erto, A. Lancia, F. Di Natale, Simultaneous absorption of SO2 and NOx from simulated flue-gas exploiting the enhancing oxidative ability of aqueous euchlorine as scrubbing solution, Fuel 368 (2024) 131611, https://doi.org/10.1016/j.fuel.2024.131611.
[8] D. Flagiello, F. Di Natale, A. Lancia, I. Sebastiani, F. Nava, A. Milicia, A. Erto, Experimental and modelling approach to the design of chemical absorption columns with fast gas-liquid reaction: a case-study on flue-gas desulfurization with H2O2 oxidative solutions, Chem. Eng. Res. Des. 194 (2023) 425–438, https://doi.org/10.1016/j.cherd.2023.04.040.
[9] D. Thomas, S. Colle, J. Vanderschuren, Designing wet scrubbers for SO2 absorption into fairly concentrated sulfuric acid solutions containing hydrogen peroxide, Chem. Eng. Technol. 26 (2003) 497–502, https://doi.org/10.1002/ceat.200390074.
[10] S. Colle, J. Vanderschuren, D. Thomas, Pilot-scale validation of the kinetics of SO2 absorption into sulphuric acid solutions containing hydrogen peroxide, Chem. Eng. Process. Process Intensif. 43 (2004) 1397–1402, https://doi.org/10.1016/j.cep.2004.04.005.
[11] F. Shokry, A. Osama, A. Salama, A. Reda, E. Noshy, M. Magdy, R. Elshafey, M. Bassyouni, R.M. Zaraa, Process simulation and design of sulfuric acid production via double contact Process, Egypt. J. Chem. 0 (2025), https://doi.org/10.21608/ejchem.2025.362901.11346, 0-0.
[12] I. Liémans, B. Alban, J.P. Tranier, D. Thomas, SOx and NOx absorption based removal into acidic conditions for the flue gas treatment in oxy-fuel combustion, Energy Proced 4 (2011) 2847–2854, https://doi.org/10.1016/j.egypro.2011.02.190.
[13] O. Okolo, Scrubbing of sulfur dioxide from secondary process gases in a copper smelter, 2021.
[14] P.S. Nolan, Flue gas desulfurization technologies for coal-fired power plants, in: Coal-Tech 2000 International Conference, 2000, pp. 1–13.
[15] S.J. Biondo, J.C. Marten, A history of flue gas desulfurization systems since 1850: research, development and demonstration, J. Air Pollut. Control Assoc. 27 (1977) 948–961, https://doi.org/10.1080/00022470.1977.10470518.
[16] U. Neumann, D. van Velzen, Sulphur dioxide and nitrogen the Wellman Lord process. Sulphur Dioxide and Nitrogen Oxides in Industrial Waste Gases: Emission, Legislation and Abatement., EurocoursesChemical Environ. Sci., 1991.
[17] A. Poullikkas, Review of design, operating, and financial considerations in flue gas desulfurization systems, Energy Technol. Policy. 2 (2015) 92–103, https://doi.org/10.1080/23317000.2015.1064794.

[18] S. Shostak, K. Kim, Y. Horbatenko, C.H. Choi, Sulfuric acid formation via H2SO3 oxidation by H2O2 in the atmosphere, J. Phys. Chem. 123 (2019) 8385–8390, https://doi.org/10.1021/acs.jpca.9b05444.
[19] S. Colle, J. Vanderschuren, D. Thomas, Effect of temperature on SO2 absorption into sulphuric acid solutions containing hydrogen peroxide, Chem. Eng. Process. Process Intensif. 47 (2008) 1603–1608, https://doi.org/10.1016/j.cep.2007.08.014.
[20] D. Flagiello, A. Erto, A. Lancia, F. Di Natale, Experimental and modelling analysis of seawater scrubbers for sulphur dioxide removal from flue-gas, Fuel 214 (2018) 254–263, https://doi.org/10.1016/j.fuel.2017.10.098.
[21] D. Flagiello, F. Di Natale, A. Erto, A. Lancia, Wet oxidation scrubbing (WOS) for flue-gas desulphurization using sodium chlorite seawater solutions, Fuel 277 (2020) 118055, https://doi.org/10.1016/j.fuel.2020.118055.
[22] R. Sander, Compilation of Henry's law constants (version 4.0) for water as solvent, Atmos. Chem. Phys. 15 (2015) 4399–4981, https://doi.org/10.5194/acp-15-4399-2015.
[23] D.W. Green, R.H. Perry, Perry's Chemical Engineers'handbook, 8th Editio, McGraw-Hill Companies, 2008.
[24] C.C. Chen, H.I. Britt, J.F. Boston, L.B. Evans, Local composition model for excess gibbs energy of electrolyte systems. Part I: single solvent, single completely dissociated electrolyte systems, AIChE J. 32 (1986) 444–454, https://doi.org/10.1002/aic.690320311.
[25] C.C. Chen, L.B. Evans, A local composition model for the excess gibbs energy of aqueous electrolyte systems, AIChE J. 32 (1986) 444–454, https://doi.org/10.1002/aic.690320311.
[26] D. Flagiello, F. Di Natale, A. Lancia, A. Erto, Characterization of mass transfer coefficients and pressure drops for packed towers with Mellapak 250.X, Chem. Eng. Res. Des. 161 (2020) 340–356, https://doi.org/10.1016/j.cherd.2020.06.031.
[27] D. Ricchiari, D. Flagiello, A. Erto, L. Amato, A. Lancia, F. Di Natale, Determination of the gas-liquid reaction kinetic for sulfur dioxide absorption in sodium chlorite aqueous solutions, Chem. Eng. Sci. 303 (2025) 120938, https://doi.org/10.1016/j.ces.2024.120938.